Proposal for PhD topic: Two Neutron Correlation Study in Photofission of Actinides

Roman Shapovalov

Physics Department at
Idaho State Univerdity

Adviser: Prof. Dan Dale

October 12, 2011

Abstract

It has well been known that two fission fragments (FF's) are emitted essentially back to back in the laboratory frame. That can be used widely in many applications as a unique signature of fissionable materials. However such fission fragments are difficult to detect. The energy and angular distributions of neutrons, on the other hand, are easily to measure, and that distribution will carry information about the fission fragments energy and angular spectra, as well as the neutron spectra in the fission fragment rest frame.

We propose to investigate the two neutron correlation yield resulting from two FF's as a function of different targets, the angle between the two neutrons and the neutron energies. The preliminary calculation of the two neutron correlation shows a huge asymmetry effect: many more neutrons are emitted anti-parallel to each other than parallel to each other. That asymmetry becomes even more if the energy cut on each neutron is done. This study will potentially permit a new technique for actinide detection for homeland security and safeguards applications as well as improve our knowledge of correlated neutron emission.

Contents

Chapter 1

Statement of the physics problems

1.1 Simple summary of fission physics

The physics of photofission is well described in many books [1, 2]. The overall process can be schematically represented as shown in Fig. 1.1. What we are going to discuss here is up to the time scale of about $10^{-14} - 10^{-13}$ sec when the prompt neutrons are emitted from the fully accelerated fragments and completely ignore all the following processes where the prompt gammas and delayed β, γ and n are emitted We will only touch on some specific information we will need to understand the underlying physics in the proposed two neutron correlational study. That mechanism is, of course, in some sense, an approximation, because we do not count possible "scission" neutrons emitted at the instant of fission [10]. What we assume here is that all neutrons are emitted from fully accelerated fission fragments.

It has long been known that the photofission reaction with a heavy nucleus in the energy range of the giant dipole resonance goes through the intermediate compound nucleus. That intermediate nucleus is in an excited state which followed by the emission of two fission fragments:

$$\gamma + A \rightarrow A^* \rightarrow FF_1 + FF_2 + TKE \tag{1.1}$$

where TKE is the total kinetic energy which will be shared by the two fission fragments. In general, the TKE will be a function of the fragment mass which has been measured by several authors [19, 20, 21, 22] as seen in the fig. 1.2. Because the fission fragments are essentially non relativistic, the TKE will be distributed proportional to their mass ratio as:

$$\frac{T_1}{T_2} = \frac{M_2}{M_1} \tag{1.2}$$

where T_1, T_2 are the kinetic energies of fragments 1 and 2 such that $TKE = T_1 + T_2$ and M_1, M_2 are their rest masses correspondingly.

The typical mass distribution at the energy range not too far from the threshold barrier is shown in the fig. 1.3 [14]. It is symmetric about $A = 120$ and for every heavy fragments there is a corresponding light one, but the fission with two equal mass fragments is less probable by a factor of about 200. It is interesting, that as the energy of incident γ's increases the masses of two FF's tend to be equal [15].

The angular distribution of individual FF's can be explained according to A.Bohr's fission channel concept [5] and briefly described by R.Ratzek et al. [11] with regards to photoinduced

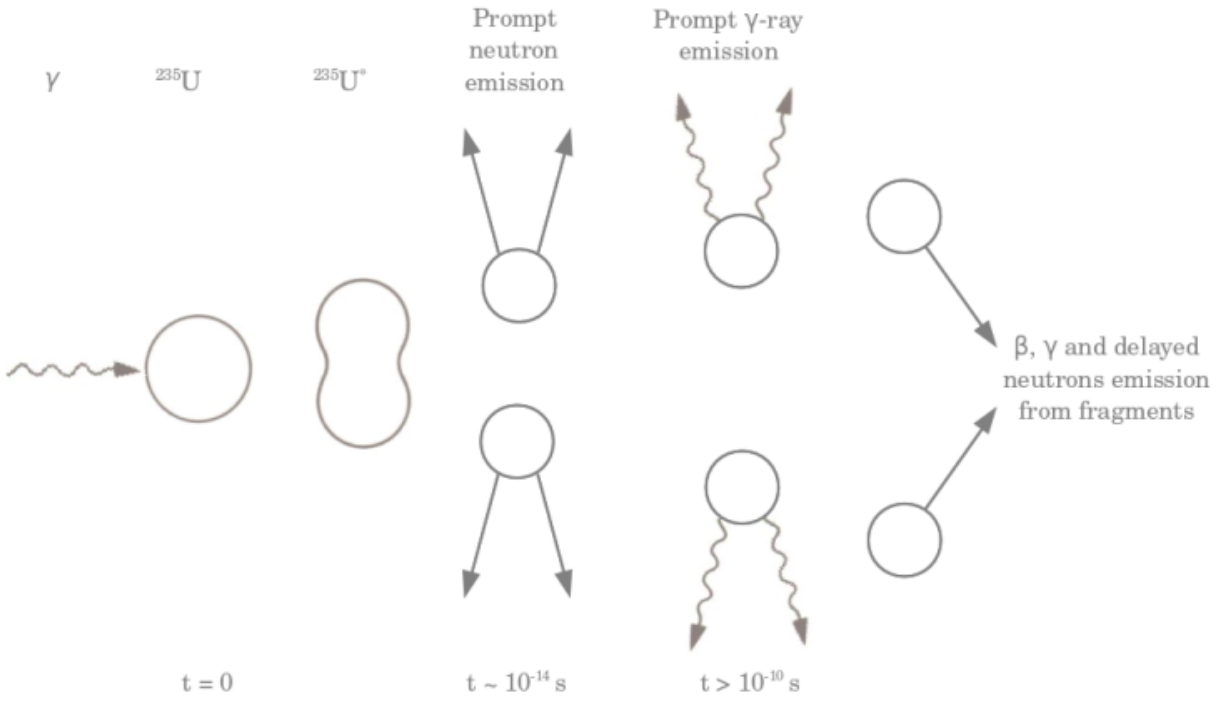

Figure 1.1: Schematic representation of the fission process in uranium. Neutrons are emitted from fully accelerated fission fragments. The time scale gives the orders of magnitude only.

reactions. If we restrict ourselves to the photofission of an even-even nucleus ($J^\pi = 0^+$, such as ^{238}U) and consider only electric dipole (E1) transactions, the angular distribution of fission fragments can be written as [11]:

$$W(\Theta) = A_0 + A_2 P_2(cos\Theta) \tag{1.3}$$

The angular distribution coefficients A_0 and A_2 depend on the transition state (J,K), where K is projection of the total spin J on the symmetry axis of the deformed nucleus. For J = 1, K = 0, we have $A_0 = \frac{1}{2}$, $A_2 = -\frac{1}{2}$ and for J = 1, K = 1, we have $A_0 = \frac{1}{2}$, $A_2 = \frac{1}{4}$. $P_2(cos\Theta) = \frac{1}{2}(2 - 3\sin^2\Theta)$ is the Legendre polynomial. Qualitatively, the angular distribution of the fission fragments can be explained if we consider the nuclear excitation as a collective motion of neutrons against the protons [4]. Because the incident gamma's are transfered wave, that will cause protons to oscillate against the neutrons in the direction of electric field **E** followed by the splitting of nucleus into the two fission fragments.

Some simple consideration of kinematics of reaction 1.1 can clarify some important moments. In the first step the incident gammas interact with heavy nucleus A resulting in compound intermediate state A*. For such step, if the energy of incident particles is small, say below or about 20 MeV, after applying the momentum conservation law, we can easily see that the excited nucleus A* is almost in rest. Because of that, and applying the momentum conservation law to the last step of reaction, we conclude that two the FF's are flying away almost in opposite direction as seen in the laboratory frame. This simple conclusion is very important and can be used widely in many applications as a unique signature of fissionable materials.

After about $10^{-14} - 10^{-13}$ sec the fission fragments will emit neutrons. As was already

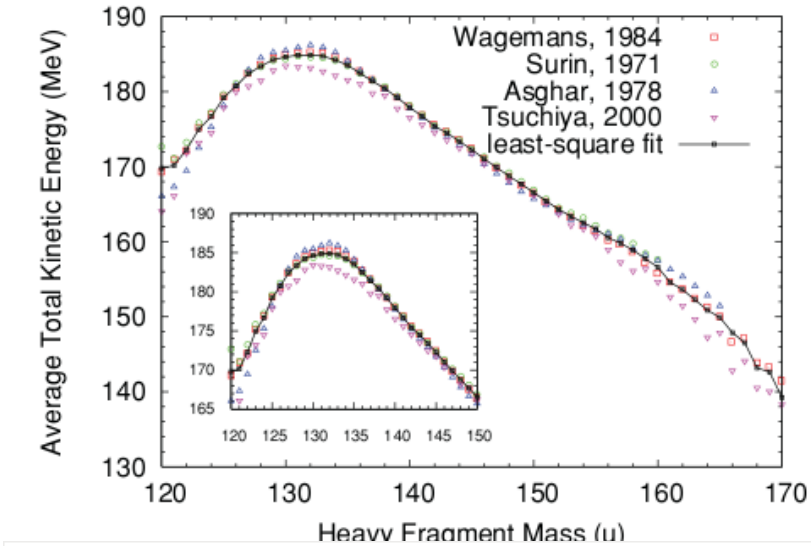

Figure 1.2: The average TKE as a function of the heavy fragment mass. The solid line is the result of a least-square fitting of the experimental data sets.

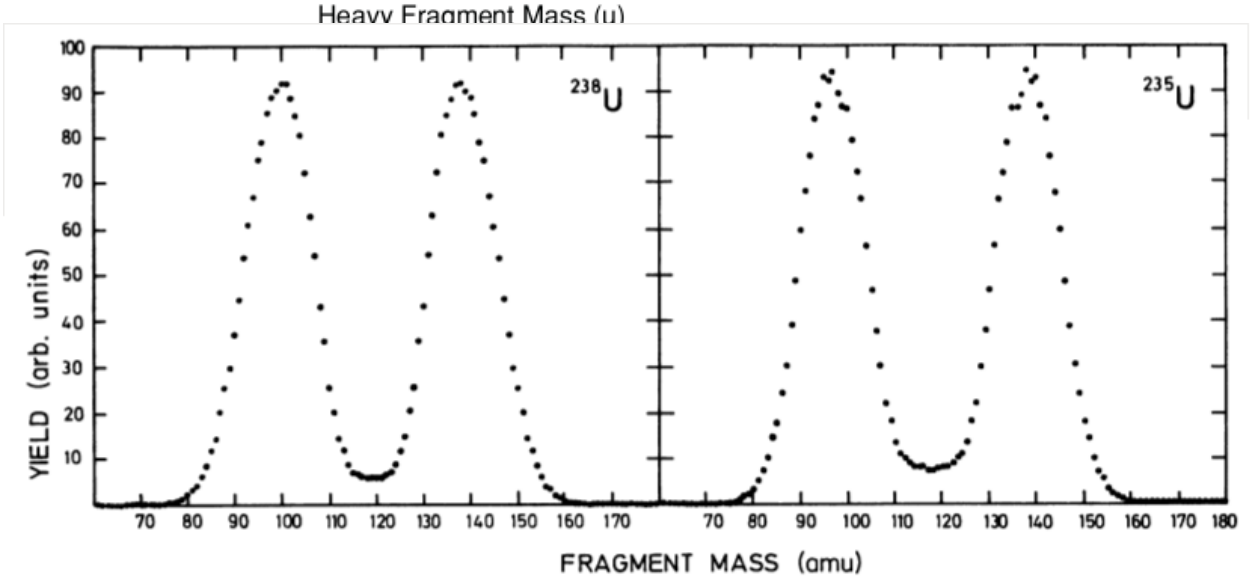

Figure 1.3: Integrated fission fragments yield (arbitrary units) versus fragment mass for the photofission of ^{238}U and ^{235}U with 25-MeV bremsstrahlung

mentioned, it was assumed that all prompt neutrons are emitted from fully accelerated fragments and there are no so called "scission" neutrons emitted at the time of fission. The important parameter to be considered here is the total excitation energy (TXE) of the intermediate nucleus A^*. That total excitation energy will be shared among light and heavy fragments and the exact form of such distribution is the open question. However, there is strong evidence [23, 24] that when the excitation energy is relatively low the light fragments will acquire the larger part of that shared energy. Those excited fission fragments can release energy and angular momentum by emitting prompt neutrons and prompt γ rays as well, but it can be assumed that the initial energy release is completely due to the neutron emission [17]. Because the excitation energy of the fission fragments is large in comparison with the lowest lying nuclear levels, the statistical model to analyze the neutron emission spectrum can be applied [3]. Using that approach, to a very good approximation, the angular distribution of prompt neutrons is isotropic in the center of mass of the fission fragments.

The energy of the evaporated neutrons can be described by the Maxwell distribution with the spectrum temperature T:

$$\rho(\epsilon_n) = \epsilon_n \exp\left(\frac{\epsilon_n}{T}\right) \tag{1.4}$$

where ϵ_n is the neutron kinetic energy in the center-of-mass fragment frame.

After the first neutron was emitted the second one will be emitted and so on until the excitation energy of the fragments becomes less then neutron separation energy. Finally, the rest of the excitation energy can be released by prompt γ ray emission. But what we assume here that only one neutron is emitted from the fully accelerated fission fragments.

Below is a short summary of the photofission reaction mechanisms discussed above which will be used in the following section to discuss the idea of the proposed two neutron correlation:

- two fission fragments recoil essentially back to back.
- the angular distribution of the prompt neutrons are isotropic in the center of mass of the fission fragments with a statistical energy distribution.
- each fully accelerated FF emits only one neutron.

1.2 Idea of 2n correlations

Let starts to count how many FF's pairs are going antiparallel and how many FF's pairs are going parallel to each other. Because two fission fragments recoil back to back, the FF's asymmetry would be, of course, infinity (there are no two FF's going parallel to each other):

$$\mathrm{A_{FF}} = \frac{\mathrm{FF's\ antiparallel}}{\mathrm{FF's\ parallel}} = \infty \tag{1.5}$$

where *FF's antiparallel* is the number of FF's pairs going in antiparallel direction and *FF's parallel* is the number of FF's pairs going in parallel direction.

The problems here is that fission fragments are very difficult to detect. For target thicker than a few mg/cm^2, due to their heavy ionization loss almost all fission fragments will stop their path inside the target. On the other side the neutrons emitted by these fission fragments will fly outside of target and could be easily detected. The question we want to study here is whether or not the angular asymmetry of fission fragments (they are always back to back) is manifest in angular distribution of prompt neutrons. So we want to study the angular and energy distribution of two neutron correlations as seen in laboratory frame with ultimate goal to calculate the two neutron asymmetry:

$$\mathrm{A_{2n}} = \frac{\mathrm{2n's\ antiparallel}}{\mathrm{2n's\ parallel}} \tag{1.6}$$

where *2n's antiparallel* is the number of 2n's pairs going in antiparallel direction and *2n's parallel* is the number of 2n's pairs going in parallel direction as seen in the LAB frame.

As we already know, the recoiling fission fragments emit neutrons isotropically in their center of mass with statistical energy distribution. If we take typical 1 MeV neutron in

the center of mass of fission fragment it will travel with the speed of about 4.6% of the speed of light. The angular distribution of neutrons in this frame will be essentially isotropic as was discussed previously. If we take two fission fragments with typical mass numbers $A_1 = 95$ and $A_2 = 143$ they will travel with the speed of about 4.6% and 3.0% of the speed of light correspondingly and they will fly away in the opposite direction. The energy and angular distribution of neutrons observed in LAB frame will be superposition of these two spectrum: 1) the spectrum of neutrons in fission fragment frame and 2) the spectrum of fission fragments.

The expected 2n correlation asymmetry could be thought as product of asymmetry of two fission fragments $\mathrm{A_{FF}}$ (f-la 1.5) times washing effect due to isotropic angular distributing of neutrons in fission fragment frame $\mathrm{W_n}$ times washing effect due to multiple Coulomb scattering inside the target and surrounding materials $\mathrm{W_{scat}}$:

$$\mathrm{A_{2n}} = \mathrm{A_{FF}} \cdot \mathrm{W_n} \cdot \mathrm{W_{scat}} \tag{1.7}$$

Because the first term is the big number we can expect that total two neutrons asymmetry as measured in laboratory frame (f-la 1.6) would be the sufficient to observe.

There are a lot of implementation of proposed here two neutron correlations technique. First of all because the expected asymmetry is large that method has a good potential to be used as good indicator of fissionable materials. In second because we can assume that angular distributions of two fission fragments with respect to each other is known exactly we in principal can calculate with very good accuracy the angular distribution of prompt neutrons as seen in the fission fragment frame to test different theories here.

Chapter 2

Brief review of what has been done

The first ever measurements of photofission fragments angular distribution was performed on Thorium in 1952 - 1954 by several authors [6, 7, 8] and was summarized and briefly discussed by Winhold and Halpern in 1956 [9]. It was found that the observed angular distribution has the form $a + b\sin^2\Theta$ (fig.2.1) and the ratio b/a depends on the energy of

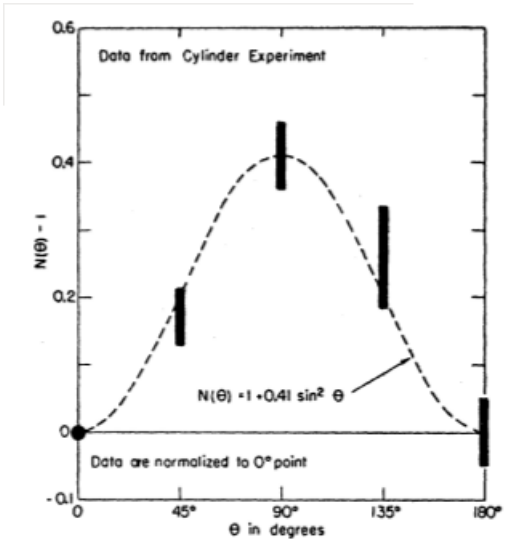

Figure 2.1: The angular distribution, $N(\Theta)$, of fission fragments from Th^{232} caught at the angles Θ to the x-ray beam. The x-ray beam was produced in a thick lead target by an electron beam whose spectrum was centered at 13 MeV and was about 5 MeV wide.

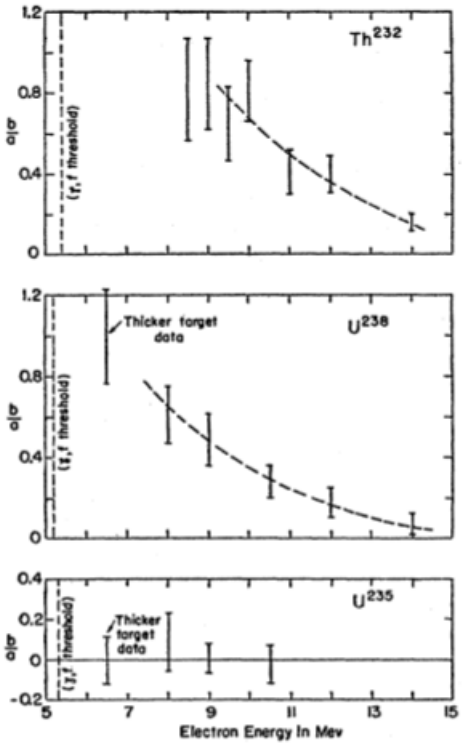

Figure 2.2: The anisotropy in the photofission of three targets. The angular distributions were all assumed to be the form $a + b\sin^2\Theta$.

the photons producing the fission, on the particular fissionable target being irradiated, and on the particular fission fragments being observed. The energy dependence of anisotropy as function of incident photon energy for tree different targets was measures and analyzed.

It was found that the photons in the giant resonance region produce essentially isotropic fission and the anisotropic fission is due solely to photons with in about 3 MeV of the fission threshold. As can been seen from fig 2.2 the anisotropies in Th^{232} and U^{238} decrease rapidly with increasing electron energy and there are no any anisotropy at all for U^{235}. That was discussed and analyzed using the Bohr model of collective motion [5].

Years later the neutron angular and energy distribution was first made by Bowman and all [10] in 1962 by analyzing the spontaneous fission of ^{252}Cf. They have used the time of flight techniques to measure the neutron angular and energy distribution in coincident with fission fragments. The measured experimental data was analyzed by assumption that there are no 'scission' neutrons and there are 10% of 'scission' neutrons. The last assumption in general gives the better agreement with the measured data as can been seen from the fig. 2.3. The energy neutron spectrum in the fission fragment rest frame presented in the

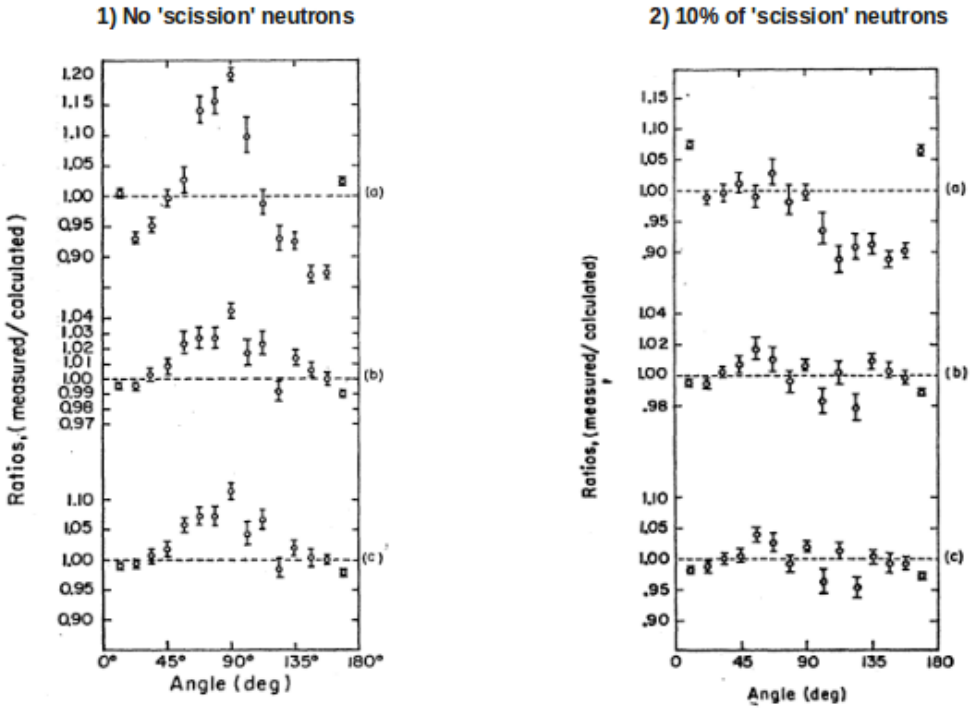

Figure 2.3: The ratio of measured to calculated values for (a) numbers of neutrons (b) average velocities, and (c) average energies as a function of angles.

fig 2.4. The large dots represent the neutrons emitted in the direction of the light fragments and the triangles represent the neutrons emitted in the direction of the heavy fragments. The smaller dots were obtained from measured neutrons emitted in the backward direction from the light fragments. The curve for light fragments was reduced by the factor 1.16, which is the ratio of the number of neutrons from the light fragments to the number from the heavy fragments. The results can be explained well by assumption of isotropic evaporation of neutrons from the fully accelerated fragments.

Further measurements of fission fragments and neutrons angular and energy distribution from the spontaneous fission of ^{252}Cf was made by Budtz-Jorgensen and Knitter in 1988 [12]. The measured neutron energy spectrum (fig. 2.5) is in a very good agreement with the

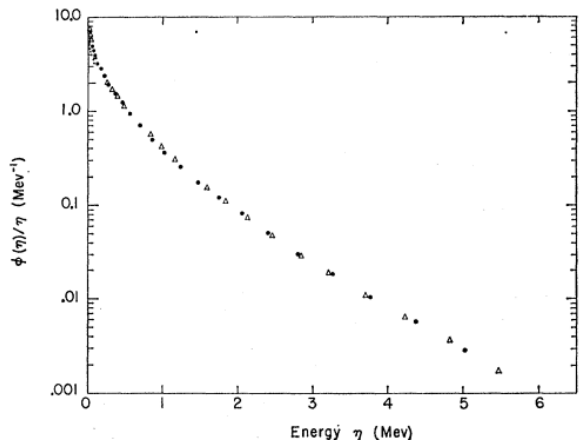

Figure 2.4: The center-of-mass neutron energy spectrum $\phi(\eta)$ (c.m) divided by η.

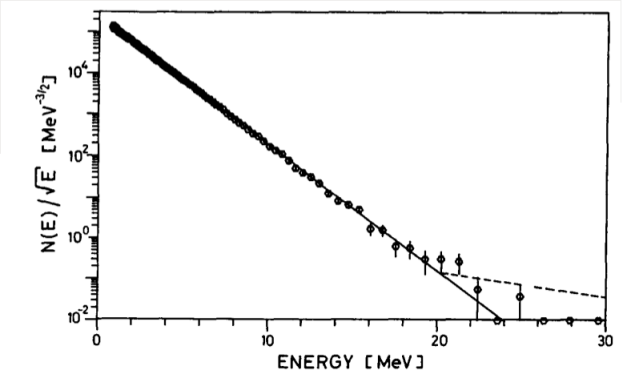

Figure 2.5: Fission neutron energy spectrum divided by the square root of the neutron energy versus the neutron energy. The solid line is Maxwell energy distribution.

Maxwell distribution in the energy range below 20 MeV energy point with the temperature parameter of $T = 1.41 \pm 0.03$ MeV. The neutron angular distribution recalculated in the fission fragment rest frame integrated over all neutron energies and normalized to unity is plotted in Fig. 2.6. The results confirm the isotropic neutrons angular distribution made by many authors in most modern theoretical models. The obtained angular anisotropy are compared by authors with data obtained by Bowman [10] as a function of fission neutron energy and is presented in fig. 2.7. There are good agreement between both measurements up to about 4 MeV and significant discrepancy above that point. The solid line is theoretical line calculated with the assumption that there are no 'scission' neutrons and is in good agreement with the Budtz-Jorgensen measurements.

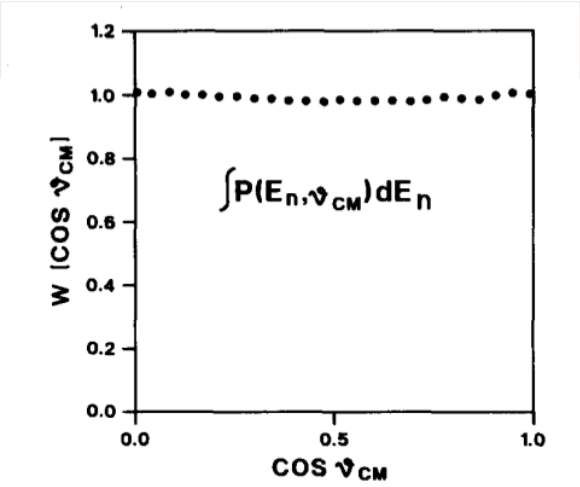

Figure 2.6: Fission neutron angular distribution in the fragment center-of-mass system integrated over all neutron energies

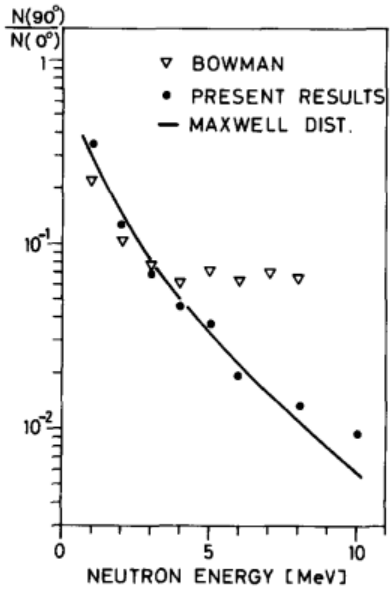

Figure 2.7: Fission neutron intensity ratio $N(90^o)/N(0^o)$ is plotted versus the fission neutron energy.

Chapter 3

Our experimental set-up

We are planning to use the HRRL LINAC to construct the beamline to produce the Bremsstrahlung photons. From Dr. Kim talk, that machine can supply the 20 ns and higher pulse width with about 10-80 mA peak current. That will give to us the necessary room to adjust the beam parameters to satisfy the desired condition to have the one fission per pulse as will be described in the following section. Because such low rate needed the main advantage of HRRL LINAC is, of course, the hight repetition beam pulse rate of 1000 Hz that will permit to increase the statistics as compared with the other machines available in IAC.

The production of unpolarized photons is the well known technique and is widely described in the literature [13]. When electrons strike the thin radiator the resulting Bremsstrahlung radiation collimated in the forward with respect to the beam direction will be unpolarized. The typical energy spectrum of Bremsstrahlung photons for the 7 MeV endpoint energy is shown in the figure 4.6.

Such beamline of unpolarized photons will be used to measure the two neutron correlation yield as function of different targets, the angle between two neutrons and the neutron energy. The time of flight (TOF) technique will be used to identify neutrons and to measure their energy, with the start signal coming from the accelerator beam pulse. The typical 1 MeV neutron is traveling with the speed of flight of about 5%. If we take the neutron detector located 1 m away from the target that will correspond to the TOF equal to:

$$\frac{1\ m}{0.05 \times 3 \cdot 10^8\ m/s} \approx 67\ ns$$

The TOF of flight of gammas scattered from the target and flying with the speed of light c will be around 3.3 ns. That will allow to distinguish neutrons from gammas. Fig. 3.1 shows the typical time of flight spectrum from photodisintegration of deuteron measured from previous HRRL runs. By converting the measured time of flight of neutrons to their velocity we will be able to reconstruct the neutron energy. Of course, the error in neutron energy will depend from the LINAC pulse width. For the machine we are going to use,the pulse width, as was mentioned above, is about 20 ns and that will limit the precision with which we will be able to measure the neutron energy. To reduce such kind of error the distance from target to detector could be increased up to about 2 m.

Because the one fission per pulse is required the neutron detectors with the big area is

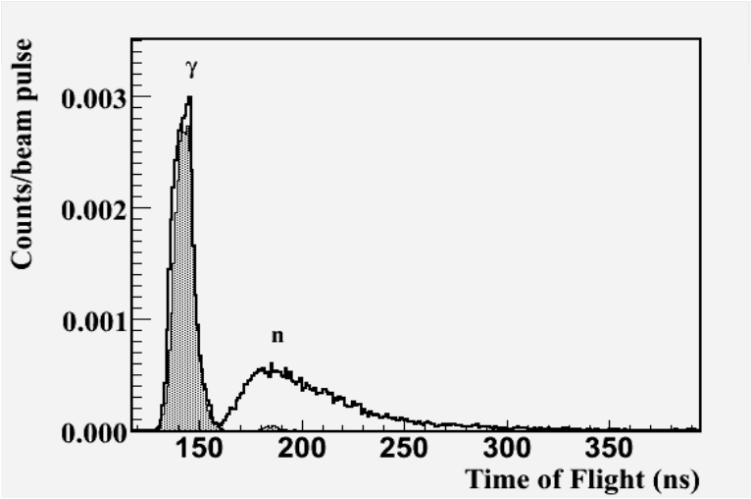

Figure 3.1: Typical TOF spectrum from photodisintegration of deuteron measured from previous HRRL runs. The distance from target to detector is about 2 m. The spectrum illustrate the ability to distinguish gammas peak from neutrons one.

needed. We currently have 16 big plastic scintillators with the size of about 15 $cm \times 88\ cm \times 3.8\ cm$ that corresponds to the front area of about 15 $cm \times 88\ cm = 0.132\ m^2$. Such plastic scintillators surrounding the target will be placed at the angle of 90 degree with respect to the beam. Because the neutrons are emitted mostly in the perpendicular to the beam direction (fig. 4.2), such geometry will allow to maximize the 2n correlation yield. Further thinking and calculation about the detector location should be done but, in principal, that will allow to almost cover the 2π geometry as can be seen from the figure 3.2. That shows only the one of the possible way of detector location and not necessary will be implemented. Two PMT will be symmetrically attached to both ends of each detector. To increase the collected light from the detector especially at the area close to the ends, the non-scintillated plastic transpared to the visible and UV light will be placed between the detector and PMT.

To be able to find the angle between two neutrons the position resolution along the length of detector is needed. Assume the neutron hits the detector at some distance y from the first PMT as shown in the figure 3.3. Two technique to find the position y can be used here.

The first method is as follow. The amplitudes A_1 and A_2 detected by PMT_1 and PMT_2 correspondingly will be proportional to distances y and $(l - y)$ the light is traveling as following:

$$A_1 = I_0 e^{-\alpha y}$$

$$A_2 = I_0 e^{-\alpha (l-y)}$$

where l is the detector length and α is the attenuation constant. If we take the natural logarithm of the ration of A_1 and A_2 the distance y where the neutron hit the detector becomes:

$$y = \frac{l}{2} - \frac{1}{2\alpha} \ln \frac{A_1}{A_2} \tag{3.1}$$

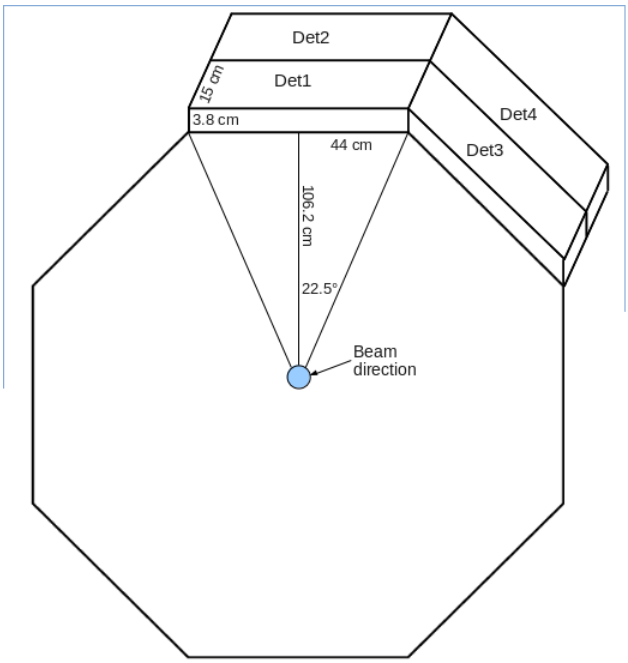

Figure 3.2: Possible detector geometry to measure the two neutron correlation yield. Total 16 neutron detectors are placed at the angle of 90 degree with respect to the beam. The detector size is 15 $cm \times 88$ $cm \times 3.8$ cm.

The other method we can use here is the timing technique. The TOF T_1 and T_2 detected by PMT_1 and PMT_2 correspondingly can be calculated as following:

$$T_1 = \frac{L}{c} + \frac{yn}{c}$$

$$T_2 = \frac{L}{c} + \frac{(l-y)n}{c}$$

where l is as before the detector length, L is distance the neutron travel from the target to detector, c is the speed of light and n is the index of reflection of scintillator material used in the detector. Taking the difference of T_1 and T_2 the position y can be found easily:

$$y = \frac{c}{2n}(T_1 - T_2) + \frac{l}{2} \tag{3.2}$$

The both techniques can be used to calculate the position where the neutron hits the detector. But the last method looks more simple and preferable in the following sense. In the first methods the amplitudes of both PMT's for each detector should be measured. To find the energy of neutron, in addition, the TOF spectrum measurements, is needed as well. The two independent channels of acquisition system is needed in that case for each PMT's. In the last timing technique method the only TOF measurements for each PMT is required. That will allow to find the position y as described by the formula 3.2 as well as the neutron

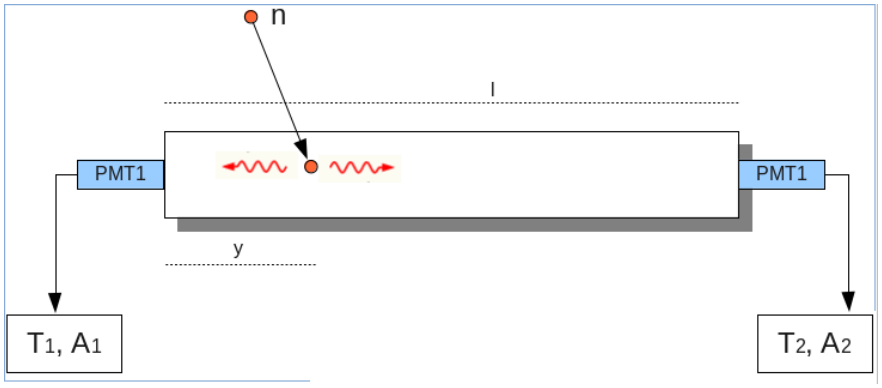

Figure 3.3: Neutron detector with two PMT attached to both ends. Neutron n hits the detector at distance y from first PMT. The amplitude signals A_1, A_2 and TOF signals T_1, T_2 are measured from PMT_1 and PMT_2 correspondingly.

energy by converting the TOF to the neutron velocity. So the only one acquisition system channel will be needed in the last case.

Some TOF measurements with 1 PMT attached to the end of detector and with ^{243}CF source moved along the detector was performed and is shown in Fig. 3.4. The results show the ability to identify the source position as function of measured TOF. The calculated speed of light inside scintillator is about 7 cm/sec that corresponds to about $n = 4$ index of reflection. Also note the minimum distance from the source to PMT where the data was collected is about 15 cm. Below that point no signal was detected. That so called 'dead zone' of detector where the light from scintillator does not go to PMT. To restore this situation some non-scintillated plastic between the end of detector and PMT as was mentioned above will be placed.

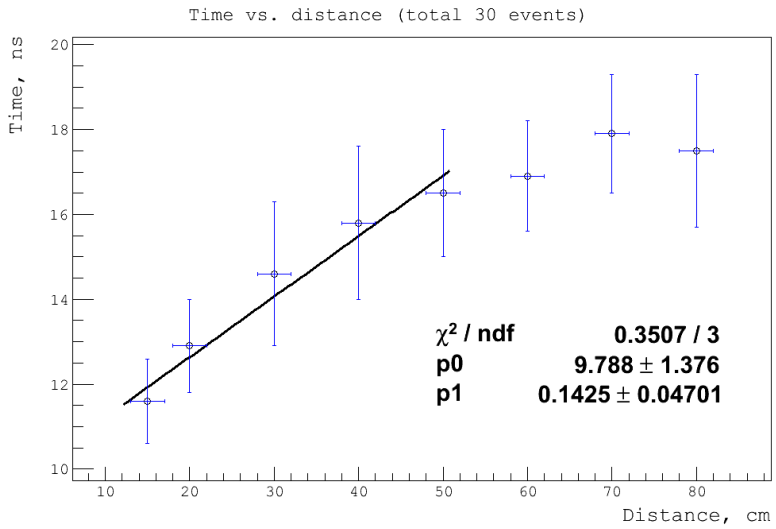

Figure 3.4: TOF measurements with 1 PMT attached to the end of detector and with ^{243}CF source moved along the detector the detector

Chapter 4

Expected results

4.1 Asymmetry calculation

To estimate the expected asymmetry in 2n correlations the Monte-Carlo simulation was performed. Total number of 10 million fission events was simulated. Each neutron was sampled up to 10 MeV in the fission fragment rest frame. The following assumptions was made:

- The fission fragment mass distribution was sampled uniformly between $85 < A < 105$ and $130 < A < 150$
- A fixed amount of total kinetic energy of 165 MeV is given to the two fission fragments and was distributed between them proportional to their mass ratio
- Each fission fragments emit one neutron. There are total two neutrons, marked as a and b for each fission event. Neutrons are emitted isotropically in the center of mass of fully accelerated FF's with the energy distribution given by:

$$N(E) = \sqrt{E} \exp\left(-\frac{E}{0.75}\right) \tag{4.1}$$

  This reproduces the laboratory neutron energy distribution as measured with (n,f) channel.

- Two recoiled fission fragments emit back to back. Fission fragments angular distribution was sampled according to:

$$W(\Theta) = \frac{1}{2} + \frac{1}{4}\left(\frac{1}{2}(2 - 3\sin^2\Theta)\right) = \frac{3}{4}\left(1 - \frac{1}{2}\sin^2\Theta\right) \tag{4.2}$$

  for $J = 1$, $K = 1$.

Note that the distribution 4.2, because there are no Φ dependence, a priory assumes the isotropic azimuthal distribution of fission fragments. That gives us the unpolarized beam of gammas interacting with target.

After both angular and energy distributions of neutrons and FF's was sampled as described above, neutrons was boosted from fission fragments rest frame into laboratory frame. The energy and direction of neutrons a and b for every fission event was recorded in the LAB frame.

To confine yourself that the simulated algorithm is correct some preliminary results of described above simulations are discussed below.

The energy spectrum of sum of kinetic energy of two neutrons a and b emitted by fully accelerated fission fragments as seen in laboratory frame is plotted in the figure 4.1:

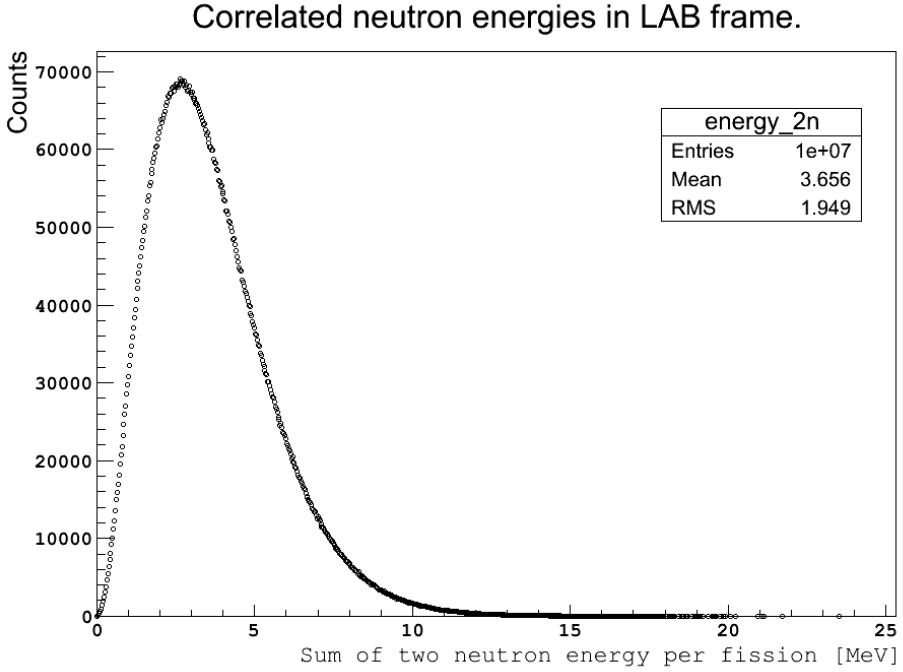

Figure 4.1: The energy distribution of sum of kinetic energy of two neutrons a and b emitted by fully accelerated fission fragments as seen in laboratory frame

Because the typical neutron energy in the fission fragment rest frame is about 1 MeV and the spectrum above is the spectrum of the sum of two neutron energies, the pick value of about 2.4 MeV looks reasonable after boost into LAB frame.

Angular distributions of prompt neutrons, as seen in laboratory frame, is presented in the figure 4.2. That is, in principal, what everyone should expect for detection of one neutron. Here the neutron a is coming from one fission fragment and the neutron b is coming from the other one as was assumed above. These angular distributions are convolution of FF's angular distribution, which is, according to f-la 4.2, strongly anisotropic and isotropic neutron angular distribution in the fission fragment rest frame. And the question which angular distribution is manifested in the resulting neutron angular distribution is important here.

First we note that angular distributions of both neutrons a and b look statistically similar as we can expect because there are no any reason for discrepancy. Also, as we can see, the resulting angular distribution is strongly anisotropic: more neutrons are emitted in perpendicular to the beam directions ($\cos\Theta = 0$) then those are in parallel ($\cos\Theta = \pm 1$). We can conclude here that anisotropy in the fission fragments angular distribution is strongly

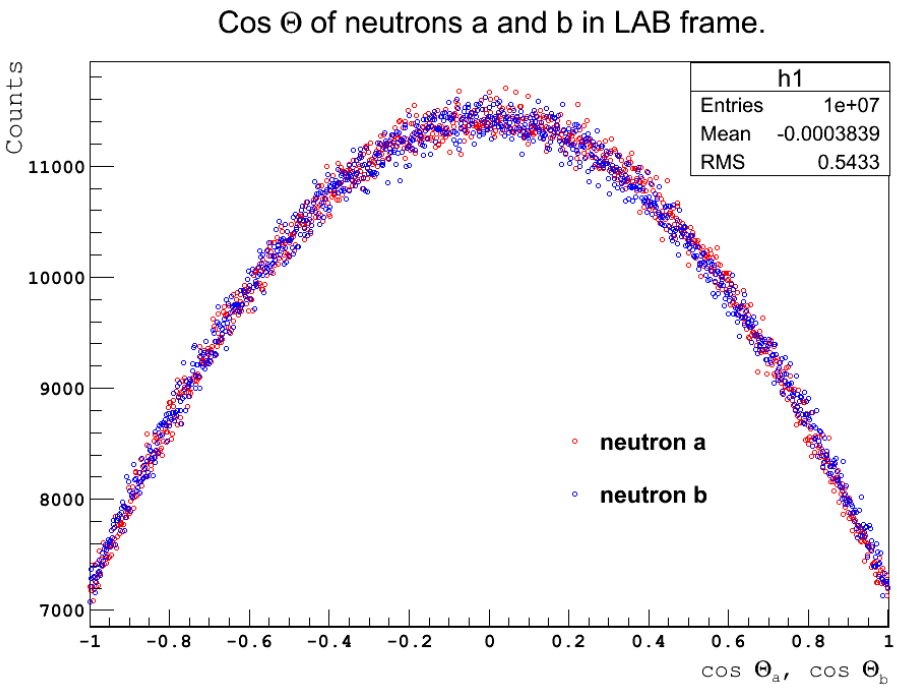

Figure 4.2: Angular distribution of prompt neutrons a (red) and b (blue) emitted by two fission fragments as seen in laboratory frame.

manifested in the angular distribution of prompt neutrons in laboratory frame. That result is important and could be used widely.

After energy and angular distributions of both neutrons a and b in the LAB frame was simulated, and we confined yourself that our simulation is sensible as was discussed just above, we can start to investigate the two neutron correlation. We can count, for example, how many of them are going in anti-parallel direction and how many are going in parallel direction with respect to each other as function of different quantities. Then the asymmetry in two neutron correlation can be calculated (see formula 1.4):

$$\mathrm{A_{2n}} = \frac{\text{2n's antiparallel}}{\text{2n's parallel}}$$

The results of two neutron correlation as function of the sum of two neutron energies is represented in the figure 4.3. To count neutron pairs are going in antiparallel and parallel directions the following assumption was made:

- two neutrons are antiparallel to each other if $\cos(\Theta_{2n}) < -0.9$
- two neutrons are parallel to each other if $\cos(\Theta_{2n}) > 0.9$

where Θ_{2n} is the calculated angle between neutrons a and b as seen in laboratory frame.

Of course, we can not count events corresponding to certain neutron energy, or to the sum of two neutron energies, as are said above. When we are saying that we are always

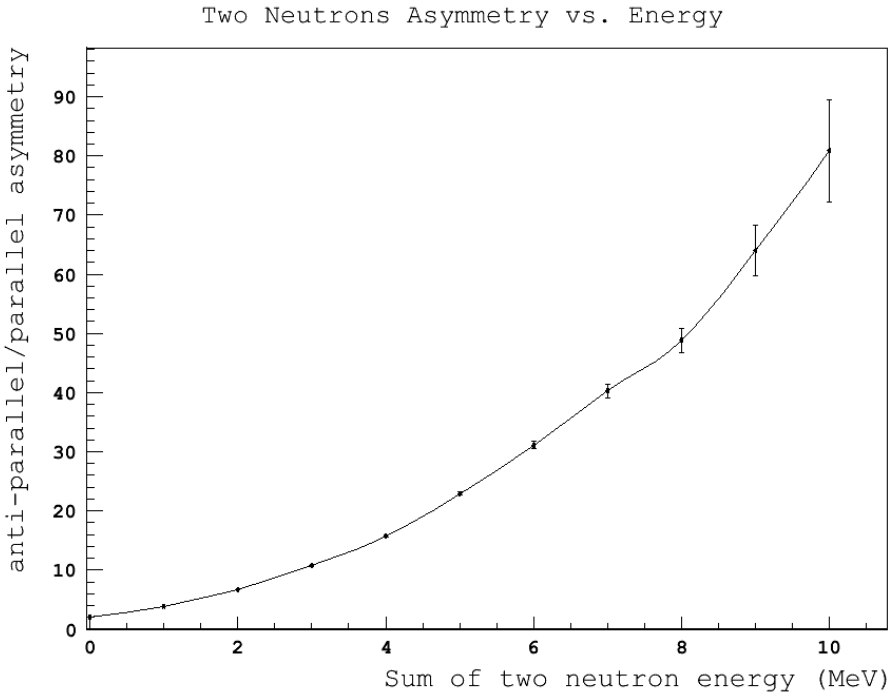

Figure 4.3: Calculated 2n asymmetry (antiparallel/parallel) as function of sum of two neutron energy

assuming some energy interval in which events was counted. The exact values of intervals was used and numerical values of calculated 2n asymmetry and different yields are shown in the table 4.1.

Table 4.1: Calculated 2n asymmetry (antiparallel/parallel) as function of sum of two neutron energy

#	(Ea+Eb), MeV	cnts_total	cnts_int	cnts180	cnts0	2n Yield	Asymm Yield	Asymm
0	0.0 + 1.0	10000000	399953	27920	13556	0.04000	0.00415	2.06 ± 0.02
1	1.0 + 1.0	10000000	1628053	142211	36695	0.16281	0.01789	3.88 ± 0.02
2	2.0 + 1.0	10000000	2238223	232958	34691	0.22382	0.02676	6.72 ± 0.04
3	3.0 + 1.0	10000000	2048413	243893	22714	0.20484	0.02666	10.74 ± 0.07
4	4.0 + 1.0	10000000	1514708	200007	12707	0.15147	0.02127	15.74 ± 0.14
5	5.0 + 1.0	10000000	976912	140562	6133	0.09769	0.01467	22.92 ± 0.30
6	6.0 + 1.0	10000000	571885	88873	2854	0.05719	0.00917	31.14 ± 0.59
7	7.0 + 1.0	10000000	312163	51793	1287	0.03122	0.00531	40.24 ± 1.14
8	8.0 + 1.0	10000000	160819	28005	574	0.01608	0.00286	48.79 ± 2.06
9	9.0 + 1.0	10000000	79827	14595	228	0.00798	0.00148	64.01 ± 4.27
10	10.0 + 1.0	10000000	37923	7201	89	0.00379	0.00073	80.91 ± 8.63

As we can see the resulting two neutron asymmetry is a strong function of the sum of two neutron energies. It increases from about 2 up to about 80 as we are going from 0 to 10 MeV energy point. Also note that as we are going to higher energy point the error becomes significant and reaches up to 10% value at the 10 MeV point. That is simple because at the higher energy range the number of counts becomes smaller. As we can see from the table 4.1, for example, in the energy point of 10 MeV the number of neutron pairs going in antiparallel direction is about 7200 and those ones going in parallel direction is only about 90. The asymmetry yield here, which is the sum of numbers of neutron pairs going in antiparallel

and parallel directions divided by the total number of events, is about 0.07%. So if we would like to study the high asymmetry values in the high energy interval, the big statistics is required. The maximum statistics of about 2.7% asymmetry yield is reached in the energy interval of about (3 - 4) MeV and the corresponding asymmetry is about 10 here. It could be noted here that asymmetry yields qualitatively follow the energy spectrum of the sum of two neutron energies presented earlier in the plot 4.1: it starts from about 0.4% asymmetry yield at 0 MeV point, reaches the maximum values of about 2.7% at the energy range of (3 - 4) MeV, and goes down up to 0.07% at 10 MeV point. The more discussion about the required statistics to run experiment is done in the following section.

Also it would be interesting to calculate the two neutron asymmetry as function of energy cut on each neutron and compare with results just presented above. Such kind of calculation is presented in the the figure 4.4 and in the table 4.2.

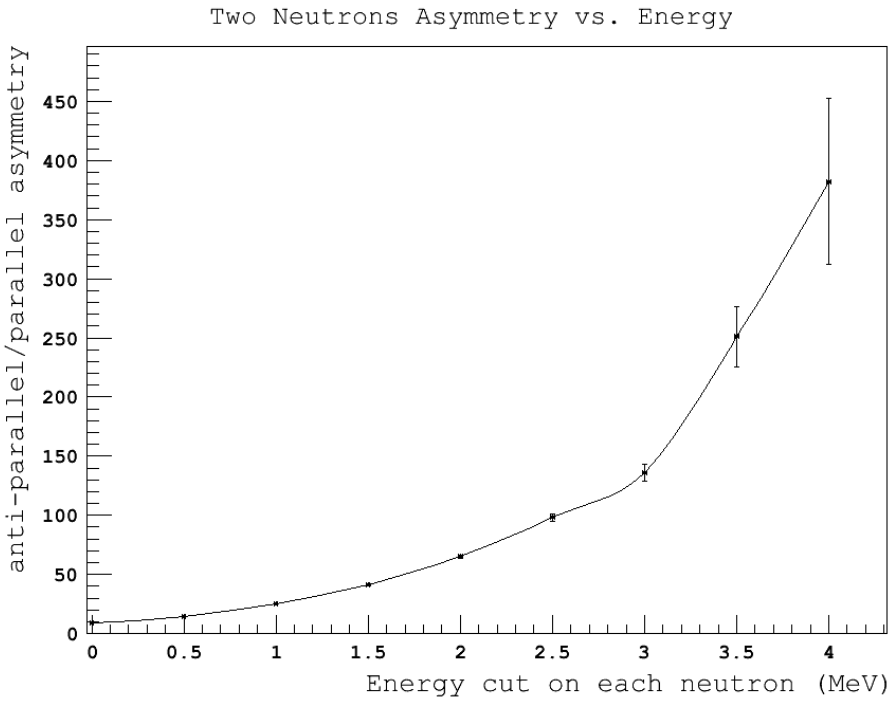

Figure 4.4: Calculated 2n asymmetry (antiparallel/parallel) as function of energy cut on each neutron

As we can see by doing, say, 1 MeV energy cut on each neutron the expected asymmetry would be of about 25, and by doing 4 MeV cut the expected asymmetry reaches the huge values of about 380. Nevertheless the problem here is as before: the more energy cut we are doing the more asymmetry error we get just because, as already was discussed, it reduces the number of counts at hight energy area. It is interesting to note that even not doing any energy cut, by counting all neutron pairs going in antiparallel and parallel directions, the expected asymmetry would be of about 9 and that corresponds to the maximum 2n asymmetry yield of about 13%.

Table 4.2: Calculated 2n asymmetry (antiparallel/parallel) as function of energy cut on each neutron

#	E_Cut, MeV	cnts_total	cnts_cut	cnts180	cnts0	2n Yield	Asymm Yield	Asymm
0	0.0	10000000	10000000	1184431	131572	1.00000	0.13160	9.00 ± 0.03
1	0.5	10000000	7356078	962173	65184	0.73561	0.10274	14.76 ± 0.06
2	1.0	10000000	4429529	642068	25642	0.44295	0.06677	25.04 ± 0.16
3	1.5	10000000	2413642	382418	9285	0.24136	0.03917	41.19 ± 0.43
4	2.0	10000000	1227505	209578	3219	0.12275	0.02128	65.11 ± 1.16
5	2.5	10000000	592912	108071	1100	0.05929	0.01092	98.25 ± 2.98
6	3.0	10000000	275153	52865	388	0.02752	0.00533	136.25 ± 6.94
7	3.5	10000000	123314	25105	100	0.01233	0.00252	251.05 ± 25.15
8	4.0	10000000	53842	11469	30	0.00538	0.00115	382.30 ± 69.89

In general, the results presented in the table 4.2 is better then those ones presented in the table 4.1 in the following sense. First note, that in the first case (table 4.1), the maximum asymmetry yield we can get is about 2.7% and that corresponds to the 2n asymmetry value of about 10. In the second case, by doing, say, 0.5 MeV energy cut on each neutron, we can easily reach asymmetry yield of about 10% and that will correspond to the 2n asymmetry value of about 15. So we get the bigger asymmetry values with the bigger asymmetry yield and with less statistical error in the second case. That conclusion, if there will be the need, can be used in future to analyze experimental data. By doing the energy cut we can significantly increase the calculated 2n asymmetry still having good statistical error.

There are several ways to make simulations presented above are more realistic. Some of them are directly following from assumptions was made in simulation algorithm:

- Use more realistic FF's mass distribution.
- Instead of 2 neutrons per fission we can use the more realistic multiplicity value.

Some other factors can be considered as well. One of them was already discussed (fla 1.5) and is due to multiple Coulomb scattering inside the target. The other factor is the geometrical neutron efficiency. That could, in principal, be calculated and should be done, when the decision about the detector geometry will be made. The third factor, is the intrinsic absolute detector efficiency, and should be measured or reasonably estimated before the experiment will start. That, of course, will decrease the calculated 2n asymmetry results.

Some advanced models [17] and experimental data [18] indicate that more neutrons are emitted from the light fragments than from heavy ones. But that implementation would be the complicated one and is good for theoretical advanced simulation programs. To our purpose, the simulated results presented here are more than enough to be interested in proposed experimental study of 2n correlation yield as function different quantities.

4.2 Counts rate calculation

It was shown in the previously section that expected 2n asymmetry (antiparallel/parallel) is a big number (f-la 1.7) and strongly depends from the sum of two neutron energies (fig. 4.3) as well as from the energy cut on each neutron (fig. 4.4). For example, we can expect the asymmetry value of about 65 doing 2 MeV cut on each neutron still having reasonable asymmetry yield of about 2%.

However, the problem arises as follow. Let assume we have N fission events per one beam pulse and let count how many two neutron coincidences are true and how many are accidental ones. The true coincidences are between two neutrons coming from the same fission event and obviously that for N fission events we will have N true coincidences. Let call them $\mathrm{N_{true}}$. The accidental coincidences are between two neutrons but coming from different fission events and as can be easily seen they are proportional to $N(N-1)$. Let call them $\mathrm{N_{accidental}}$. Now let calculate the following ratio:

$$\frac{\mathrm{N_{true}}}{\mathrm{N_{accidental}} + \mathrm{N_{true}}} = \frac{N}{N(N-1)+N} = \frac{1}{N} \tag{4.3}$$

To be able to observe the true coincidences we want the ratio above to be equal to one. The only way to do it is to make $N = 1$. That will guarantee that every coincidence will be a priory a true one with no way to have the accidental one. So we need to design the experiment in such way that the following condition will be satisfied:

$$\mathrm{N} = \frac{\text{1 fission event}}{\text{pulse}} \tag{4.4}$$

Let do some count rate calculation to check the possibility to satisfy to the condition above. By taking $\tau = 20\ ns$ pulse width and $I = 20\ mA$ peak current the number of electrons per pulse will be:

$$N_{e^-} = 20 \cdot 10^{-3} \frac{\text{Coloumb}}{\text{sec}} \times \frac{1\ \mathrm{e^-}}{1.6 \cdot 10^{-19}\ \text{Coloumb}} \times 20\ \text{ns} = 2.5 \cdot 10^9\ \frac{\mathrm{e^-}}{\text{pulse}} \tag{4.5}$$

To be specific, let use the ^{235}U as a target. The figure 4.5 shows (γ, f) and $(\gamma, 2n)$ photo-nuclear cross sections as function of incident photon energy [25]. As we can see the optimal photon energy would be about 6-7 MeV. In that case the (γ, f) cross section will be the low one, which is good, with no way to have the '2n knockout' because we well below the threshold energy of about 12 MeV for the $(\gamma, 2n)$ channel. So by choosing the 7 MeV electron beam energy, we will be able to study the pure (γ, f) channel.

The bremsstrahlung spectrum with 7 MeV endpoint energy for the thin Al radiator is shown in the figure 4.6 [**?**]. That will produce of about 0.05 photons/$\mathrm{e^-}$/MeV/r.l. in the 6-7 MeV region.

Taking the thickness of Al radiator equal to 90 microns (about 10^{-3} radiation length), the number of bremsstrahlung photons going out of radiator in the 6-7 MeV energy range can be calculated as follow:

$$N_{\gamma'} = 2.5 \cdot 10^9\ \frac{\mathrm{e^-}}{\text{pulse}} \times 0.05\ \frac{\text{photons}}{\mathrm{e^-}\ \text{MeV r.l.}} \times 1\ \text{MeV} \times 10^{-3}\ \text{r.l.} = 1.25 \cdot 10^5\ \frac{\gamma'\text{s}}{\text{pulse}} \tag{4.6}$$

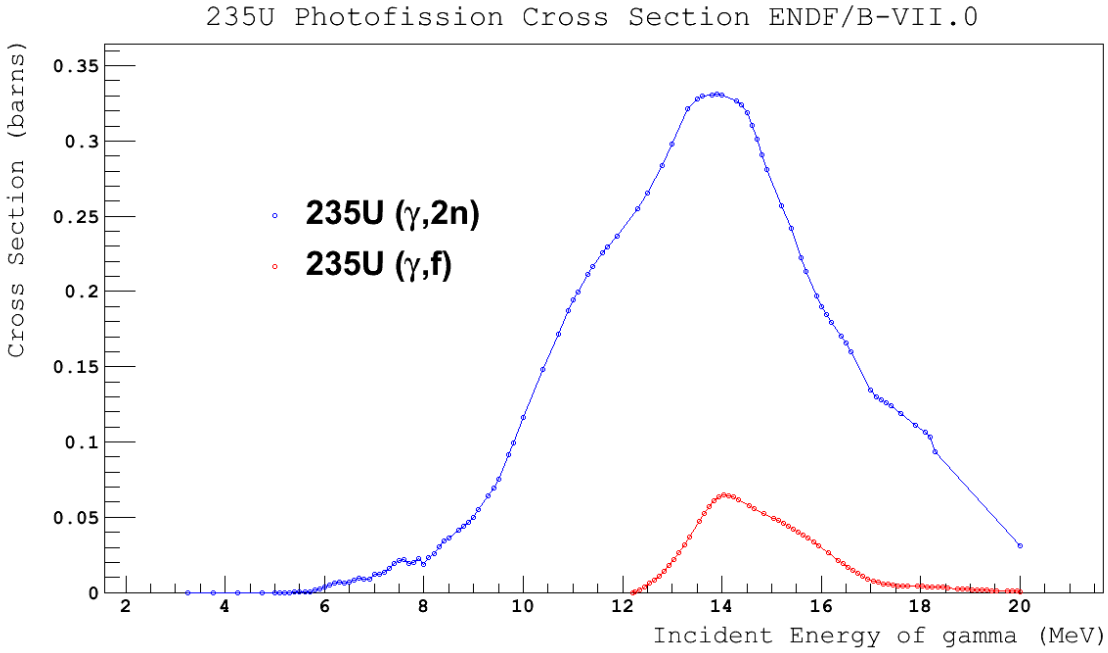

Figure 4.5: ^{235}U photofission cross section taken from ENDF/B-VII.0

Not all photons calculated above will hit the target. Some of them will be lost due to collimation. Assuming the collimation factor is about 50%, the number of photons hitting the target becomes:

$$N_\gamma = \mathrm{N}_{\gamma'} \times 50\% = 6.25 \cdot 10^4 \ \frac{\gamma' \mathrm{s}}{\mathrm{pulse}} \tag{4.7}$$

We want the one fission per pulse. That can be found by adjusting the target thickness from the equation below:

$$\frac{1 \text{ fission}}{\text{pulse}} = N_\gamma \times t \times \sigma \tag{4.8}$$

where t the is the target thickness in atoms/cm^2 and the σ is the $(\gamma, 2n)$ photo-nuclear cross section and is about 7 mb/atom in the 6-7 MeV energy range as can be seen from the figure 4.5 above. The thickness becomes:

$$\mathrm{t} \ \left[\frac{\text{atoms}}{\mathrm{cm}^2}\right] = \frac{1 \frac{\text{fission}}{\text{pulse}}}{6.25 \cdot 10^4 \ \frac{\gamma' \mathrm{s}}{\text{pulse}} \times 7 \ \frac{\text{mb}}{\text{atom}}} = 2.29 \cdot 10^{21} \ \frac{\text{atoms}}{\mathrm{cm}^2} \tag{4.9}$$

that could be converted into the cm as follow:

$$t \ [cm] = \frac{\mathrm{t} \cdot \mathrm{M}}{\rho \cdot \mathrm{N_A}} = \frac{2.29 \cdot 10^{21} \ \frac{\text{atoms}}{\mathrm{cm}^2} \times 235.04 \ \frac{\mathrm{g}}{\text{mol}}}{19.1 \ \frac{\mathrm{g}}{\mathrm{cm}^3} \times 6.02 \cdot 10^{23} \ \frac{\text{atoms}}{\text{mol}}} = 470 \ \mu\mathrm{m} \tag{4.10}$$

where M is the molar mass, ρ is the density of ^{235}U and N_A is the Avogadro number.

In the last step we was be able by varying the target thickness to satisfy the desired situation of having the one fission per pulse. In principal, the other element of beam line,

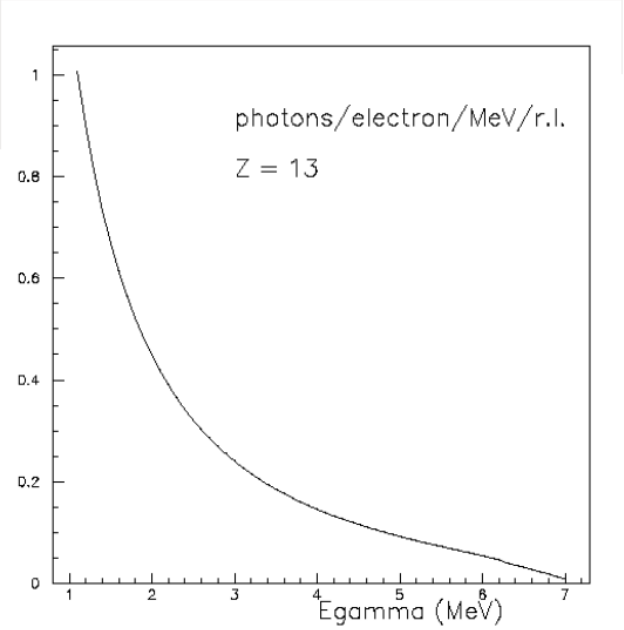

Figure 4.6: Bremsstrahlung spectrum of photons produced by 7 MeV electrons hitting the Al radiator

like radiator thickness or collimation factor, can be varied as well. After the reasonable judgment about the beam line elements will be done, we still have the possibility to adjust count rates by varying the LINAC beam parameters, such as the electron pulse width and the electron peak current.

4.3 Beam time calculation

Let estimate the time needed to run experiment. As was already mentioned in the previous section to eliminate the accidental coincidence the one fission per pulse rate is required and because that condition the Hight Repetition Rate Linac (HRRL) available at IAC will be a good choice.

Let calculate the coincidence rate we would expect for two neutron detectors located 2 m away from the target as presented in the fig 4.7.

The count rate for both detectors can be calculated as:

$$\mathrm{N}\ \left[\frac{\mathrm{coinc}}{\mathrm{sec}}\right] = \frac{1\ \mathrm{fission}}{\mathrm{pulse}} \cdot \mathrm{N_G^2} \cdot \mathrm{N_{intr}^2} \cdot \mathrm{N_{cut}} \cdot 2.2 \cdot 10^3\ \mathrm{Hz} \tag{4.11}$$

where $\mathrm{N_G}$ is the geometrical detector efficiency, $\mathrm{N_{intr}}$ is the absolute intrinsic detector efficiency, $\mathrm{N_{cut}}$ is the efficiency of the energy cut, 2.2 is the average number of neutrons per fission, 10^3 Hz is the HRRL repetition rate.

The geometrical detector efficiency $\mathrm{N_G}$ is just the solid angle as the target see the detector and can be calculated as following:

$$\Omega = \frac{\mathrm{S}}{4\pi \mathrm{r}^2} = \frac{(15 \times 88)\ \mathrm{cm}^2}{4\pi (2\ \mathrm{m})^2} = \frac{0.132\ \mathrm{m}^2}{50.258\ \mathrm{m}^2} = 2.6 \cdot 10^{-3}\ \mathrm{sr} \tag{4.12}$$

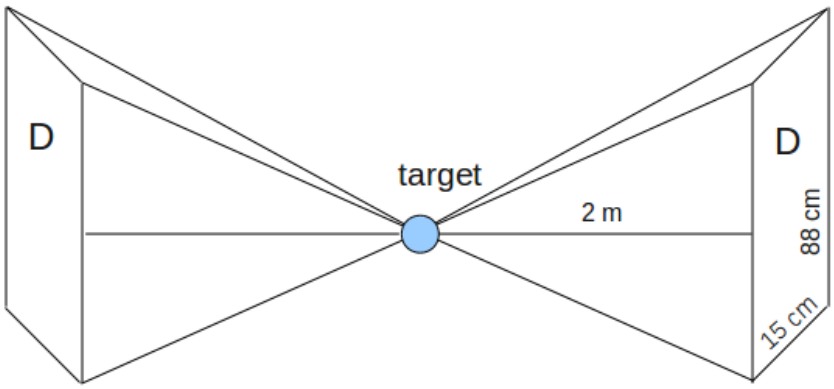

Figure 4.7: Two detector geometry located 2 m away from target

.

The intrinsic detector efficiency N_{intr} can be conservatively assumed to be about 25%. The efficiency of energy cut N_{cut} can be estimated from the table 4.2 and for 1 MeV energy cut is about 44%. Substituting all values above in the formula 4.11 the count rate for two detectors becomes:

$$N = \frac{1 \text{ fission}}{\text{pulse}} \cdot (2.6 \cdot 10^{-3})^2 \cdot (0.25)^2 \cdot 0.44 \cdot 2.2 \cdot 10^3 \text{ Hz} = 4 \cdot 10^{-4} \frac{\text{coinc}}{\text{sec}} \tag{4.13}$$

There are total 16 neutron detectors available for that experiment that will increase the count rate by the factor of $8 \times 8 = 64$ so the count rate for 16 detectors becomes:

$$N_{16 \text{ det}} = N \times 64 = 2.6 \times 10^{-2} \frac{\text{coinc}}{\text{sec}} \tag{4.14}$$

The expected statistics for 1 working day of beam time (8 hours) will be:

$$N_{day} = N_{16 \text{ det}} \times 60 \text{ sec} \times 60 \text{ min} \times 8 \text{ hours} \approx 750 \frac{\text{coinc}}{\text{day}} \tag{4.15}$$

that is good enough to analyze the experimental data.

Chapter 5

Summary, conclusion

Below are the short summary and conclusion of proposed here two neutron correlation study:

- There is a needs in experimental data of two neutron correlation measurements in fission.
- The preliminary calculation of two neutrons correlation shows the huge asymmetry effect: much more neutrons are emitted anti-parallel to each other then parallel to each other. That asymmetry becomes even more if the energy cut on each neutron will be done. There are some factors, as multiple Coulomb scattering, for example, that will reduce the calculated asymmetry and could be calculated later. But that will not reduce the expected asymmetry significantly.
- We propose to measure and analyze the two neutrons correlation yield resulting from two FF's as function of different targets, angle between two neutrons and neutron energies by utilizing well developed at IAC the bremsstrahlung photons production techniques. There are total 16 'big' plastic detectors which can be used for neutron detection. With 1000 Hz High Repetition Rate Linac available at IAC we can reach statistics of about 750 coincidences per day.
- This study will permit to create a new technique for actinide detection as well as to improve our knowledge of correlating neutron emission.

Bibliography

[1] K.S. Krane, *IBntroductory Nuclear Physics*, John Wiley & Sons, Inc., New York, 1988.

[2] S.S.M. Wong, *Introductory Nuclear Physics*, John Wiley & Sons, Inc., New York, 1988.

[3] V.Weisskopf, *"Statistics and Nuclear Reactions"*, Phys. Rev. **52**, 295 (1937).

[4] M.Goldhaber and E.Teller, *"On Nuclear Dipole Vibrations"*, Phys. Rev. **74**, 1046–1049 (1948).

[5] A.Bohr, *On the theory of nuclear fission*, Proc. 1st UN Int. Conf. on peaceful uses of atomic energy, Vol 2, 151, New York 1956.

[6] E.J.Winhold, P.T.Demos, and I.Halpern, Phys. Rev. **85**, 728(A) (1952)

[7] E.J.Winhold, P.T.Demos, and I.Halpern, *"The Angular Distribution of Fission Fragments in the Photofission of Thorium"*, Phys. Rev. **87**, 1139–1140 (1952)

[8] A.W.Fairhall, I.Halpern, and E.J.Winhold, *"Angular Anisotropy of Specific Thorium Photofission Fragments"*, Phys. Rev. **94**, 733–734 (1954)

[9] E.J.Winhold and I.Halpern, *"Anisotropic Photofission"*, Phys. Rev. **103**, 990–1000 (1956)

[10] H.R. Bowman, S.G. Thompson, J.C.D. Milton, and W.J. Swiatecki, *Velocity and Angular Distributions of Prompt Neutrons from Spontaneous Fission of* Cf^{252}, Phys. Rev., **126**, 2120 (1962).

[11] R. Ratzek, W. Wilke, J. Drexler, R. Fischer, R. Heil, K. Huber, U. Kneissl, H. Ries, H. Ströher and R. Stock, et al., *Photofission with linearly polarized photons* , Z.Phys.A - Atom and Nuclei **308**, 63 (1982).

[12] C.Budtz-Jorgensen and H.-H.Knitter, *Simultaneous investigation of fission fragments and neutrons in* ^{252}Cf *(SF)*, Nucl. Phys. **A490**, 307 (1988).

[13] U.E.P. Berg and U. Kneissl, Ann. Rev. Nucl. Part. Sci. **37**, 33-69 (1987).

[14] A. De Clercq, E. Jacobs, D. De Frenne, H. Thierens, P. D'hondt, and A. J. Deruytter, *Fragment mass and kinetic energy distribution for the photofission of* ^{235}U *and* ^{238}U *with 25-MeV end-point bremsstrahlung*, Phys. Rev. C **13**, 1536 (1976).

[15] E.Jacobs, A.De Clercq, H.Thierens, D.De Frenne, P.D'hondt, P.De Gelder, and A.J.Deruytter. *Fragment mass and kinetic energy distributions for the photofission of ^{235}U with 12-, 15-, 20-, 30-, and 70-MeV bremsstrahlung*, Phys. Rev. C **24**, 1795–1798 (1981)

[16] W.Wilke, U.Kneissl, Th.Weber and all., *Photofission of ^{238}U with monochromatic gamma rays in the energy range 11–16 MeV*, Phys. Rev. C **42**, 2148–2156 (1990)

[17] Talou, P. and Becker, B. and Kawano, T. and Chadwick, M. B. and Danon, Y. *Advanced Monte Carlo modeling of prompt fission neutrons for thermal and fast neutron-induced fission reactions on ^{239}Pu*, Phys. Rev. C, **83**, 064612 (2011).

[18] V. F. Apalin, Yu.N. Gritsyuk, I. E. Kutikov, V. I. Lebedev, and L. A. Mikaelian, Nucl. Phys. **71**, 553 (1965).

[19] C.Wagemans, E.Allaert, A.Deruytter, R.Barthélémy, and P.Schillebeeckx, *Comparison of the energy and mass characteristics of the $^{239}Pu(n_{th}, f)$ and the $^{240}Pu(sf)$ fragments*, Phys. Rev. C **30**, 218 (1984).

[20] V.M.Surin, A.I.Sergachev, N.I.Rezchikov, B.D.Kuz'minov *"Yields and kinetic energies of fragments in the fission of U233 and Pu239 by 5.5- and 15-MeV neutrons"*, Yad. Fiz. **14**, 935 (1971).

[21] C.Tsuchiya, Y.Nakagome, H.Yamana, H.Moriyama, K.Nishio, I.Kanno, K.Shin, and I.Kimura, *"Simultaneous Measurement of Prompt Neutrons and Fission Fragments for $^{239}Pu(n_{th}, f)$"*, J. Nucl. Sci. Technol. **37**, 941 (2000).

[22] M.Asghar, F.Caitucoli, P.Perrin, and C.Wagemans, *"Fission fragment energy correlation measurements for the thermal neutron fission of ^{239}Pu and ^{235}U"*, Nucl. Phys. A **311**, 205 (1978).

[23] P.Talou, T.Kawano, O.Bouland, J.E.Lynn, P.Möller, and M.B.Chadwick Proceedings of the International Conference on Nuclear Data for Science & Technology ND2010, April 26–30, 2010, Jeju Island, Korea.

[24] K.-H. Schmidt and B. Jurado. *"Entropy Driven Excitation Energy Sorting in Superfluid Fission Dynamics"*, Phys. Rev. Lett. **104**, 212501 (2010).

[25] *National Nuclear Data Center*, http://www.nndc.bnl.gov/